

Comparative microRNA Profiling of Prostate Carcinomas with Increasing Tumor Stage by Deep Sequencing

Martin Hart¹, Elke Nolte², Sven Wach², Jaroslaw Szczyrba¹, Helge Taubert², Tilman T. Rau³, Arndt Hartmann³, Friedrich A. Grässer¹, and Bernd Wullich²

Abstract

MicroRNAs (miRNA) posttranscriptionally regulate gene expression and are important in tumorigenesis. Previous deep sequencing identified the miRNA profile of prostate carcinoma versus nonmalignant prostate tissue. Here, we generated miRNA expression profiles of prostate carcinoma by deep sequencing, with increasing tumor stage relative to corresponding nonmalignant and healthy prostate tissue, and detected clearly changed miRNA expression patterns. The miRNA profiles of the healthy and nonmalignant tissues were consistent with our previous findings, indicating a high fidelity of the method employed. In the tumors, quantitative real-time PCR (qRT-PCR) analysis of 40 paired samples of prostate carcinoma versus normal tissue revealed significant upregulation of *miR-20a*, *miR-148a*, *miR-200b*, and *miR-375* and downregulation of *miR-143* and *miR-145*. Hereby, *miR-375* increased from normal to organ-confined tumors (pT2 pN0), slightly decreased in tumors with extracapsular growth (pT3 pN0), but was then expressed again at higher levels in lymph node metastasizing (pN1) tumors. The sequencing data for *miR-375* were confirmed by Northern blotting and qRT-PCR. The regulation for other selected miRNAs could, however, not be confirmed by qRT-PCR in individual tumor stages. *MiR-200b*, in addition to *miR-200c* and *miR-375* reduced the expression of *SEC23A*. Interestingly, *miR-375*, found by sequencing in pT2 upregulated by us and others in tumor versus normal tissue, and *miR-15a*, found by sequencing in pT2 and pT3 and in the metastasizing tumors, target the phosphatases PHLPP1 and PHLPP2, respectively. PHLPP1 and PHLPP2 dephosphorylate members of the AKT family of signal transducers, thereby inhibiting cell growth. Coexpression of *miR-15a* and *miR-375* resulted in downregulation of PHLPP1/2 and strongly increased prostate carcinoma cell growth.

Implications: These genomic data reveal relevant miRNAs in prostate cancer that may have biomarker and therapeutic potential. *Mol Cancer Res*; 12(2); 250–63. ©2013 AACR.

Introduction

Prostate carcinoma is the second most frequently diagnosed malignancy and a leading cause of cancer-related death in men worldwide (1). The underlying mechanisms resulting in invasive growth after dissemination of the primary tumor from the initial site in the prostate are not completely understood. MicroRNAs (miRNAs) are now recognized as contributing factors to the induction, growth, and metastasis

of most tumors, including prostate carcinoma (for a review, see refs. 2 and 3). miRNAs are short, noncoding RNAs of approximately 19–25 nucleotides that bind preferentially to specific sequences in the 3'-untranslated region (3'UTR) of mRNAs, resulting in either translational repression or mRNA degradation. Interaction of the miRNAs with their mRNA target ultimately leads to reduced protein synthesis via association with the Argonaute (Ago-) containing RNA-induced silencing complex (for a review, see ref. 4).

We have previously established the miRNA profiles of prostate carcinoma in comparison with adjacent nonmalignant prostate tissue by a deep sequencing approach. We found that 33 miRNAs were deregulated more than 1.5-fold in the cancer samples (16 miRNAs upregulated, 17 downregulated; ref. 5; for a recent review on miRNA expression analysis in prostate carcinoma, see refs. 3, 6, 7). We subsequently showed that the levels of *miR-375*, *miR-143*, and *miR-145* may be used as biomarkers to classify prostate carcinoma samples (8). On the basis of the sequence analysis, we have shown that myosin VI, which is induced in prostate carcinoma, is a target for the downregulated miRNAs *miR-145* and *miR-143*. Furthermore, the *SEC23A* mRNA is a target for the induced *miR-200c* and *miR-375* with

Authors' Affiliations: ¹Department of Virology, Saarland University Medical School, Homburg/Saar; ²University Clinic of Urology; and ³Department of Pathology, Friedrich-Alexander-University, Erlangen-Nürnberg, Erlangen, Germany

Note: Supplementary data for this article are available at Molecular Cancer Research Online (<http://mcr.aacrjournals.org/>).

M. Hart, E. Nolte, F.A. Grässer, and B. Wullich contributed equally to this work.

Corresponding Author: Friedrich Grässer, Saarland University Medical School; Department of Virology, Kirrbergerstrasse, Haus 47, 66421 Homburg/Saar, Germany. Phone: 49-6841-1623983; Fax: 49-6841-1623980; E-mail: Graesser@uks.eu

doi: 10.1158/1541-7786.MCR-13-0230

©2013 American Association for Cancer Research.

concomitant protein downregulation of SEC23A protein in prostate carcinoma. Accordingly, the overexpression of *Sec23A* resulted in reduced growth of prostate cancer cell lines (9). In addition, the downregulated miRNA *miR-24* targets the *ZNF217* mRNA; the subsequently induced ZNF217 protein is a known oncogene in other tumors and probably also plays a role in prostate carcinoma (10 and references therein).

As an extension of our recent analyses, we now compared nonmalignant prostate tissue with organ-confined tumors (pT2, pN0), tumors with extracapsular growth (pT3, pN0), and lymph node metastasizing (pN1) prostate carcinoma. We found that several of the previously identified upregulated miRNAs like *miR-375* are strongly upregulated in the pT2/pT3 tumors and even more in lymph node metastasizing prostate carcinoma (pN1). By sequencing, *miR-200b* was upregulated in the pT2 to pT3 (pN0) samples but then showed reduced levels in the metastasizing tumors. This finding was confirmed by Northern blot analysis of the pooled RNAs used for the generation and sequencing of the miRNA cDNA libraries. However, by quantitative real-time PCR (qRT-PCR) analysis, this miRNA was also increased in the pN1 samples. Furthermore, we show that *SEC23A* is also a target for *miR-200b* (in addition to *miR-200c* and *miR-375*), and that the *SEC23A* expressed in prostate carcinoma is inversely correlated to the *miR-200b/c* levels. Importantly, we identify the PHLPP1 and PHLPP2 mRNAs as targets for *miR-15a* and *miR-375*. Both *miR-15a* and *miR-375* were found induced in all tumor stages compared with normal tissue by sequencing and Northern blotting, but the increase could not be confirmed by qRT-PCR for *miR-15a*. The Pleckstrin homology domain and leucine rich repeat protein phosphatase (PHLPP) enzymes dephosphorylate the AKT kinase, which, in the phosphorylated state, induces cell growth. Loss of, or reduction of, PHLPP1 or PHLPP2 and the ensuing increase in phosphorylation of AKT is an established cause for induction and/or progression of prostate carcinoma (11–13). *MiR-15a* and *miR-375*, therefore, play important roles in prostate carcinoma and may represent potential therapeutic targets. Furthermore, miRNAs hold the potential of being valuable biomarkers for the stratification of prostate carcinoma patients into clinically relevant risk groups.

Materials and Methods

Clinical samples

This study was approved by the local ethical review board and was performed according to the Declaration of Helsinki. Tissue samples were provided by the tissue biorepository at the University Cancer Center at the University Hospital of Erlangen. Only samples containing >70% tumor cells were included in the study. Gleason score, pathologic tumor stage, histologic diagnosis, and tumor-node metastasis classification was performed according to the guidelines of the Union International Contre le Cancer 2002 (14). The samples were reviewed by an experienced uropathologist (TTR) to confirm tissue identity, tumor cell content, and the absence of tumors cells in normal tissue preparation.

For the deep sequencing analysis, pooled normal and tumor tissue samples were used. The pool of organ-confined prostate carcinoma contained 10 tumor samples (pT2, pN0), prostate carcinoma with extracapsular growth contained seven samples (pT3, pN0), and the pool of lymph node metastasized prostate carcinoma contained three samples (pN1). Corresponding nonmalignant tissue from the same organ was prepared for all prostate carcinoma samples. An additional set of normal prostate tissue was prepared from five patients undergoing radical cystectomy for bladder cancer. The pathological review confirmed the absence of tumor cells in these samples.

A second, independent cohort of 40 cryoconserved tumor tissue samples with corresponding nonmalignant tissue was used for the validation of the sequencing results. The median age of the patients at the time of diagnosis was 67 years (51–77 years). The Gleason score of these tumors ranged from 5 to 9. The nonmalignant tissue, as defined by histologic examination, was prepared from the same organ as the tumor tissue. Clinical and pathologic characteristics of patients are summarized in Supplementary Table S1.

Illumina sequencing

A total of 45 tissue samples were pooled in five groups: Normal prostate, normal prostate adjacent to prostate carcinoma, pT2 prostate carcinoma, pT3 prostate carcinoma (pN0), and pN1 prostate carcinoma, and then the small RNA fractions were isolated to generate five cDNA libraries. The isolation of small RNA, sample preparation, next generation sequencing, and bioinformatic sequence analyses were carried out by Vertis Biotechnologie AG. In short, the total RNA preparations were examined by capillary electrophoresis, the small RNA samples were separated on denaturing 15% polyacrylamide gels, and the small RNA fractions containing RNAs with a length of 19–29 bases were eluted and used for the generation of the five cDNA libraries. These cDNA pools were sequenced on the Illumina HiSeq2000 system. The sequencing reads were mapped against miRBase V.15 using CLC workbench (CLC bio). Cross-mapped reads were randomly assigned to one of all possible cross-mapping locations. For the analysis of miRNA expression, a low expression cutoff was applied when then level of a given miRNA was below 0.1% in all four libraries analyzed. For the identification of deregulated miRNAs, we applied a 1.5-fold differential expression cutoff.

RNA extraction

Extracts from primary prostate carcinoma tissues were generated using TRIzol (Life Technologies). Extraction of total RNA and protein was carried out according to the manufacturer's instructions.

Northern blotting

For Northern Blotting of the cell lines, total RNA was prepared using peqGOLD TriFast reagent (Peqlab) and used as described in the manufacturer's manual. All RNA samples were separated in a 12% denaturing urea-polyacrylamid gel and transferred to nylon membrane Hybond

N (Amersham) by semidry electro blotting (30 minutes, 15 V; ref. 10). After chemical cross-linking of the RNA for two hours at 55°C, the radioactively labeled RNA probes were hybridized overnight on the target miRNAs. The synthesis and labeling of the radioactive miRNA probes was performed according to the manufacturer's manual of miRVana Probe Construction Kit (Ambion). After washing the membrane twice for 15 minutes with 5× saline sodium citrate (SSC) and 1% SDS, and twice for 15 minutes with 1× SSC and 1% SDS, the membrane was exposed for at least 24 hours on a storage phosphor screen. The following day the phosphor screen was analyzed with the PhosphoImager Typhoon (Amersham). Stripping of the nylon membrane was carried out using Stripping Buffer (5 mmol/L Tris pH 8; 0.2 mmol/L EDTA; 0.05% NaPP; 0.1% Denhardt's solution) for 2 hours at 80°C. The sequences of RNA probes are shown in Supplementary Table S2.

miRNA qRT-PCR

For miRNA analysis, 10 ng of total RNA was reverse transcribed using the TaqMan miRNA Reverse Transcription Kit with the miRNA-specific RT primers contained in the TaqMan MicroRNA Assays (Life Technologies). RT-PCR was performed with the StepOnePlus Real-Time PCR System (Life Technologies) using sequence-specific primers and fluorescently labeled probes for *miR-200b*, *miR-200c*, *miR-375*, *miR-145*, *miR-143*, *miR-148a*, *miR-15a*, *miR-20a*, *miR-93*, and *let-7c* (Life Technologies). The PCR reactions were performed in triplicate in a final volume of 10 µL containing 1× TaqMan Universal PCR Master Mix (No AmpErase UNG), 1× TaqMan miRNA assay, and miRNA-specific primed cDNA, corresponding to an input amount of 330 pg total RNA per RT-PCR reaction. The thermal cycling conditions were as follows: 95°C for 20 seconds followed by 40 cycles of 95°C for one second and 60°C for 20 seconds. To quantify the miRNA expression in the tumor tissues, we used the relative quantification ($\Delta\Delta C_t$) method (13) with *RNU6b* serving as an internal control. RNA from PNF or LNCaP cells was always analyzed in parallel on the same reaction plate, and the expression of examined miRNAs in PNF or LNCaP cells was arbitrarily set to one. RNA from LNCaP served as the reference sample for miRNAs *miR-375*, *miR-148a*, *miR-200b*, *miR-20a*, and *miR-15b*. RNA from PNF cells served as the reference sample for miRNAs *let-7c*, *miR-145*, and *miR-143*. All calculations were performed with the StepOne software V 2.0 (Life Technologies).

qRT-PCR analysis of mRNA expression

cDNA synthesis was performed with the DyNAmo cDNA Synthesis Kit (Finnzymes Oy) using 200 ng of total RNA and random hexamer primers. The PCR primers for *PHLPP1* (fwd 5'-GTC TCC AAG GTT GCA TCC CA-3', rev 5'-GAA GAG GTT GGC AGG CAG AT-3'), *PHLPP2* (fwd 5'-GAC GGC AAT ACT CCC TTG CT-3', rev 5'-ACT CGG CCA AAG TCT CGA AG-3'), and *GAPDH* (fwd 5'-CAT GAG AAG TAT GAC AAC AGC CT-3', rev

5'-AGT CCT TCC ACG ATA CCA AAG T-3') were purchased from Biomers (biomers.net). RT-PCRs were performed in triplicate with the StepOnePlus Real-Time PCR System (Life Technologies) in a total volume of 10 µL, which contained 1× TaqMan Fast SYBR Green Master Mix (Life Technologies), 250 nmol/L forward primer, 100 nmol/L reverse primer, and 5 ng of cDNA with the following conditions: 95°C for 5 minutes, followed by 40 cycles of 95°C for 3 seconds and 60°C for 30 seconds. mRNA expression was quantified using the $\Delta\Delta C_t$ using *GAPDH* as the internal control mRNA, and RNA from PNF for normalization.

Cell lines and tissue culture

The human 293T and the human prostate carcinoma cell lines DU145 and LNCaP cells were obtained from the German Collection of Microorganisms and Cell Cultures (DSMZ). The PNF cells represent normal prostate fibroblasts and were kindly provided by Prof. Gerhard Unteregger (Department of Urology, University of Saarland Medical School, Saarland, Germany). The identity of the cell lines had previously been confirmed by the Genomics and Proteomics Core facility of the German Cancer Research Center, Heidelberg, Germany. Cells were cultured as described previously (5).

Plasmids

The pSG5-*miR-15a* expression vector was cloned by PCR amplification of nucleotides 50623080–50623503 from chromosome 13 (NC_000013.10) and ligation of the resulting fragment into the *EcoRI* and *BamHI* restriction sites of the pSG5 plasmid (Stratagene). To obtain the pSG5-*miR-200b* expression construct, the nucleotides 1102390–1102757 of chromosome 1 (NC_000001.10) were amplified by PCR with specific primers and inserted into the pSG5 expression vector. The pSG5-*miR-375* expression vector was described previously (9). The dual luciferase reporter plasmid pMIR-RNL, the pMIR-RNL-*SEC23A* reporter vector, and the appropriately mutated pMIR-RNL-*SEC23A* reporter constructs were described elsewhere (9). The nucleotides 39–905 of the *PHLPP1* 3'UTR (accession number: NM_194449.3) and the nucleotides 1–968 of the *PHLPP2* 3'UTR (accession number: NM_015020.2) were amplified via PCR using specific primers from testis cDNA and inserted via the *SpeI*, *SacI*, or *NaeI* restriction sites in pMIR-RL. The mutagenesis of the predicted target site seed sequences of pMIR-RL reporter constructs were performed with Quick-Change Site Directed Mutagenesis Kit (Stratagene), following the instructions of the manufacturer's manual. The sequences of primers used for cloning and site-directed mutagenesis are shown in Supplementary Table S2.

Dual-luciferase assays, transfections, and Western blotting

The Dual-luciferase assays were performed as described elsewhere (5) using the Dual-Luciferase Reporter Assay System in accordance with the manufacturer's instructions (Promega). For transfection of prostate carcinoma cell lines,

approximately 2×10^5 LNCaP or DU145 cells per well were seeded out in 6-well plates. After 24 hours, the prostate carcinoma cells were transfected with 2 μ g of plasmid DNA using jetPRIME (Polyplus Transfection). After 48 hours, cells were lysed with $2 \times$ sample buffer (130 mmol/L Tris/HCl, 6% SDS, 10% 3-mercapto-1,2-propanediol, 10% glycerol, and 0.05% bromophenol blue). Thirty μ g of extracted proteins were separated by 8.5% SDS-PAGE and transferred to a nitrocellulose membrane (Whatman, GE Healthcare) by Western blotting. The primary antibodies included anti-SEC23A monoclonal rat antibody 2H4-11 (5), anti-PHLPP1 (A300-661A; Bethyl Laboratories), anti-PHLPP2 (A300-660A; Bethyl Laboratories), and anti-GAPDH (Clone 14C10, NEB Cell signaling). Appropriate secondary antibodies were purchased from Sigma. Bands were visualized by enhanced chemiluminescence (Roth) with Amersham Hyperfilm ECL (GE Healthcare Europe GmbH). Western blots were quantified by Quantity One analysis software (Bio-Rad).

Cell proliferation assay

In 6-well plates, 2×10^5 DU145 or LNCaP cells per well were seeded out. After 24 hours, the cells were transfected with 2 μ g of plasmid DNA using jetPRIME (Polyplus transfection) or with 1.5 μ g miRNA inhibitor (Qiagen) using HiPerFect transfection reagent (Qiagen) based on the manufacturer's instructions. For all transfections, appropriate negative controls were included. In addition, at the 0-hour time point, the cells were harvested. At 24, 48, and 72 hours posttransfection time points, the remaining cells were collected and counted by Flow Cytometry using FACS-Canto II (BD Biosciences).

Data analysis and statistical methods

Statistical evaluation of the luciferase assays was performed with SigmaPlot 10 (Systat). Statistical analyses of real-time qRT-PCR experiments (Kruskal–Wallis test) and of cell proliferation experiments (two-way ANOVA) were performed using GraphPad Prism 6.0 (Graph Pad software). All statistical tests were performed as two-sided with P values < 0.05 considered as significant.

Results

miRNA profiling of normal prostate tissues and prostate carcinoma at various stages of malignancy

We performed miRNA-expression profiling of nonmalignant prostate tissue and prostate carcinoma at various stages of malignancy by deep sequencing. We additionally compared the miRNA expression between corresponding nonmalignant prostate tissue adjacent to prostate carcinoma and healthy prostate tissue that was derived from patients undergoing radical cystectomy due to bladder cancer. An initial analysis indicated that none of the minor transcript miRNAs (termed *-miRNAs in miRBase V.15) would withstand the applied low expression and differential expression cutoffs. Therefore all of the *-miRNAs were excluded from further analyses. The results of the

deep sequencing analysis (covering only major miRNA transcripts) are shown in Supplementary Table S3. The relative expression levels of the miRNAs were comparable and also matched the results of our previous study of healthy prostate tissue (5). The profiling of the two pools of nonmalignant prostate tissue yielded comparable results for the samples from the corresponding nonmalignant part of the prostate and healthy prostate tissue obtained after radical cystectomy. Furthermore, the relative abundance of miRNAs in the nonmalignant tissue pools was essentially the same as described in our earlier analysis (5), in which the 30 most abundant miRNAs were present at the same relative level in all three libraries, indicating that the method yields reproducible results. In the following paragraphs, we refer to healthy or normal prostate tissue adjacent to prostate carcinoma.

Next, the normal tissue samples were compared with organ-confined prostate carcinoma (pT2, pN0), prostate carcinoma with extracapsular growth (pT3, pN0), and prostate carcinoma with local lymph node metastases (pN1). Figure 1 shows the miRNAs that were up- or downregulated at least 1.5-fold in one of the tumor samples. Most miRNAs that were previously found to be induced (5) were again upregulated; most notable were the miRNAs *miR-375*, *miR-200b/c*, *miR-148a*, *miR-141*, *miR-106a/b*, *miR-21*, and *miR-20a*, whereas some like *let-7a/f* remained unchanged in the present analysis. The strongest induction was noted for *miR-375*, with the highest relative levels in the metastasized samples (pN1) as compared with the other tumor samples (pT2, pN0; pT3, pN0). Likewise, *miR-148b* and *miR-21* showed a strong upregulation in the metastasizing versus nonmetastasized tumors. This is depicted in Fig. 1A. Table 1 lists the miRNAs that displayed more than 1.5-fold change within two libraries. The complete set of data is given in Supplementary Table S3, which lists all miRNAs that were present in at least one of the libraries with a relative amount of sequence alignments of 0.1%. Interestingly, some miRNAs like *miR-200b*, *miR-200c*, *miR-25*, *miR-106a*, *miR-17*, or *miR-93* showed increasing miRNA expression levels from healthy to pT2 (pN0) to pT3 (pN0) samples but then a reduction in the lymph node metastasizing tumors. Likewise, the relative expression levels of several upregulated miRNAs like *miR-93*, *miR-18a*, *miR-20a*, or *miR-20b* were decreased in lymph node metastasizing samples compared with the amounts detected in normal samples. These results were confirmed by Northern blot analysis of the RNA samples used for the generation of the library. Notably, *let-7b* and *let-7c*, the latter previously described to be induced in medium grade prostate carcinoma (15, 16), were further upregulated in the pT3 (pN0) cases but then reduced below the levels of normal prostate in the lymph node metastasizing tumors (Fig. 1).

The strongest relative downregulation was observed for *let-7e* and *miR-205* (Fig. 1B). A strong downregulation of *miR-205* in prostate carcinoma was also observed by Boll and colleagues (17). We again noted reduced levels of miRNAs like *miR-143*, *miR-145*, *miR-320a*, or *miR-424* as previously described (5). In comparison with our previous profiling, some miRNAs, such as *miR-223*, *miR-221*, or *miR-27a*, remained unchanged in this analysis.

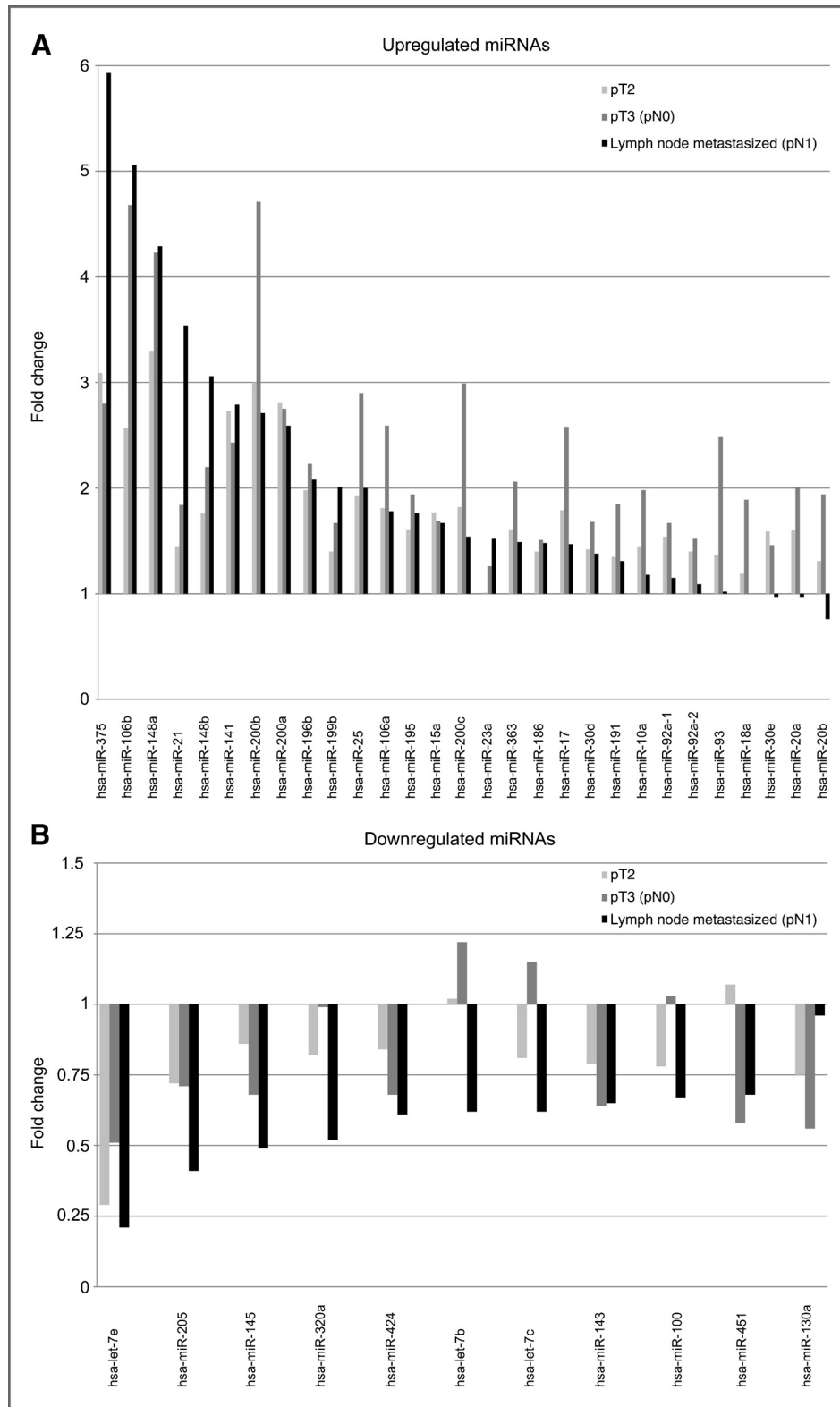


Figure 1. Expression pattern of up- and downregulated miRNAs in organ-confined (pT2, pN0), extracapsular growing (pT3, pN0), and lymph node metastasizing (pN1) prostate carcinoma. A, 29 miRNAs were found to be induced at least 1.5-fold in one tumor stage. B, 11 miRNAs are downregulated at least 1.5-fold in the tumor tissues.

Downloaded from <http://aacrjournals.org/mcr/article-pdf/12/2/250/3136432/250.pdf> by guest on 22 April 2025

Next, we selected eight miRNAs for further validation. The most pronounced up- or downregulation was observed for *miR-375* and *let-7e*. *miR-143* and *miR-145* are well-

known tumor suppressor miRNAs and a reduced expression of these miRNAs has been described multiple times (reviewed in ref. 3). miRNAs *miR-20a* and *miR-200b*

Table 1. Deregulated miRNAs identified by deep sequencing in organ-confined (pT2, pN0), extracapsular growing (pT3, pN0), and lymph node metastasizing (pN1) prostate carcinoma

Upregulated miRNAs						
miRNA	pT2 (pN0)		pT3 (pN0)		Lymph node metastasized (pN1)	
	Relative expression, %	Fold change	Relative expression, %	Fold change	Relative expression, %	Fold change
hsa-miR-106a	0.08	1.81	0.11	2.59	0.08	1.78
hsa-miR-106b	0.14	2.57	0.25	4.68	0.27	5.06
hsa-miR-10a	0.07	1.45	0.10	1.98	0.06	1.18
hsa-miR-141	3.89	2.73	3.47	2.43	3.98	2.79
hsa-miR-148a	0.94	3.30	1.20	4.23	1.22	4.29
hsa-miR-148b	0.07	1.76	0.08	2.20	0.12	3.06
hsa-miR-15a	0.94	1.77	0.89	1.69	0.89	1.67
hsa-miR-17	0.30	1.79	0.44	2.58	0.25	1.47
hsa-miR-186	0.16	1.40	0.17	1.51	0.17	1.48
hsa-miR-18a	0.08	1.19	0.13	1.89	0.07	1.00
hsa-miR-191	0.53	1.35	0.72	1.85	0.51	1.31
hsa-miR-195	0.48	1.61	0.57	1.94	0.52	1.76
hsa-miR-196b	0.09	1.98	0.11	2.23	0.10	2.08
hsa-miR-199b	0.26	1.40	0.30	1.67	0.37	2.01
hsa-miR-200a	0.31	2.81	0.30	2.75	0.28	2.59
hsa-miR-200b	0.20	3.00	0.32	4.71	0.18	2.71
hsa-miR-200c	0.55	1.82	0.90	2.99	0.46	1.54
hsa-miR-20a	0.89	1.60	1.12	2.01	0.54	0.97
hsa-miR-20b	0.19	1.31	0.28	1.94	0.11	0.76
hsa-miR-21	2.00	1.45	2.52	1.84	4.86	3.54
hsa-miR-23a	0.65	1.01	0.81	1.26	0.98	1.52
hsa-miR-25	0.18	1.93	0.28	2.90	0.19	2.00
hsa-miR-30d	0.20	1.42	0.24	1.68	0.20	1.38
hsa-miR-30e	0.13	1.59	0.12	1.46	0.08	0.97
hsa-miR-363	0.27	1.61	0.34	2.06	0.25	1.49
hsa-miR-375	1.13	3.09	1.03	2.80	2.17	5.93
hsa-miR-92a-1	0.15	1.54	0.17	1.67	0.11	1.15
hsa-miR-92a-2	0.12	1.40	0.13	1.52	0.10	1.09
hsa-miR-93	0.39	1.37	0.71	2.49	0.29	1.02

Downregulated miRNAs						
miRNA	pT2 (pN0)		pT3 (pN0)		Lymph node metastasized (pN1)	
	Relative expression, %	Fold change	Relative expression, %	Fold change	Relative expression, %	Fold change
hsa-let-7b	1.19	1.02	1.41	1.22	0.71	0.62
hsa-let-7c	0.71	0.81	1.00	1.15	0.54	0.62
hsa-let-7e	0.04	0.29	0.07	0.51	0.03	0.21
hsa-miR-100	0.47	0.78	0.63	1.03	0.41	0.67
hsa-miR-130a	0.17	0.75	0.12	0.56	0.21	0.96
hsa-miR-143	31.61	0.79	25.82	0.64	25.95	0.65
hsa-miR-145	1.27	0.86	1.00	0.68	0.73	0.49
hsa-miR-205	0.16	0.72	0.15	0.71	0.09	0.41
hsa-miR-320a	0.10	0.82	0.12	0.99	0.06	0.52
hsa-miR-424	0.24	0.84	0.19	0.68	0.17	0.61
hsa-miR-451	0.20	1.07	0.11	0.58	0.13	0.68

NOTE: miRNAs listed were deregulated by at least 1.5-fold compared with the normal tissue. Relative expression refers to the percentage of miRNA deep sequencing reads in the respective cDNA library.

exhibited the regulation pattern of stage-specific increasing expression with a dramatic reduction of expression in lymph node metastasizing prostate carcinoma. We, furthermore, selected miRNAs *miR-15a* and *miR-148a* because the functional role of these miRNAs in primary prostate carcinoma cases is currently under discussion (18–20).

The changes in the expression levels of *let-7c*, *miR-15a*, *miR-20a*, *miR-143*, *miR-145*, *miR-148a*, *miR-200b*, and *miR-375* observed by sequencing were analyzed by Northern blot analysis of the pooled RNAs employed in the generation of the cDNA libraries for sequencing as shown in Supplementary Fig. S1. We also carried out a qRT-PCR analysis for miRNAs *let-7c*, *miR-15a*, *miR-143*, *miR-145*, and *miR-148a* in 40 pairs of prostate carcinoma and corresponding nonmalignant samples.

There were significantly different expression levels for *miR-143*, *miR-145*, *miR-148a*, *miR-20a*, *miR-200b*, and *miR-375* ($P = 0.008$; $P < 0.001$; $P < 0.001$; $P = 0.020$; $P = 0.019$; $P < 0.001$; Kruskal–Wallis test) but not for *miR-15a* and *let-7c* ($P = 0.320$ and $P = 0.451$; Kruskal–Wallis test) at comparing prostate carcinoma and the corresponding normal nonmalignant sample (Supplementary Fig. S2). The quantification of the Northern blots and the corresponding qRT-PCR data from the above mentioned 40 primary tumor samples are shown in Fig. 2. The Northern blots partially reflect the changes in expression levels obtained by sequencing, in particular, for *miR-375*, which showed an increase from normal to pT2, a slight decrease from pT2 (pN0) to pT3 (pN0), and a strong additional increase from pT3 (pN0) to the

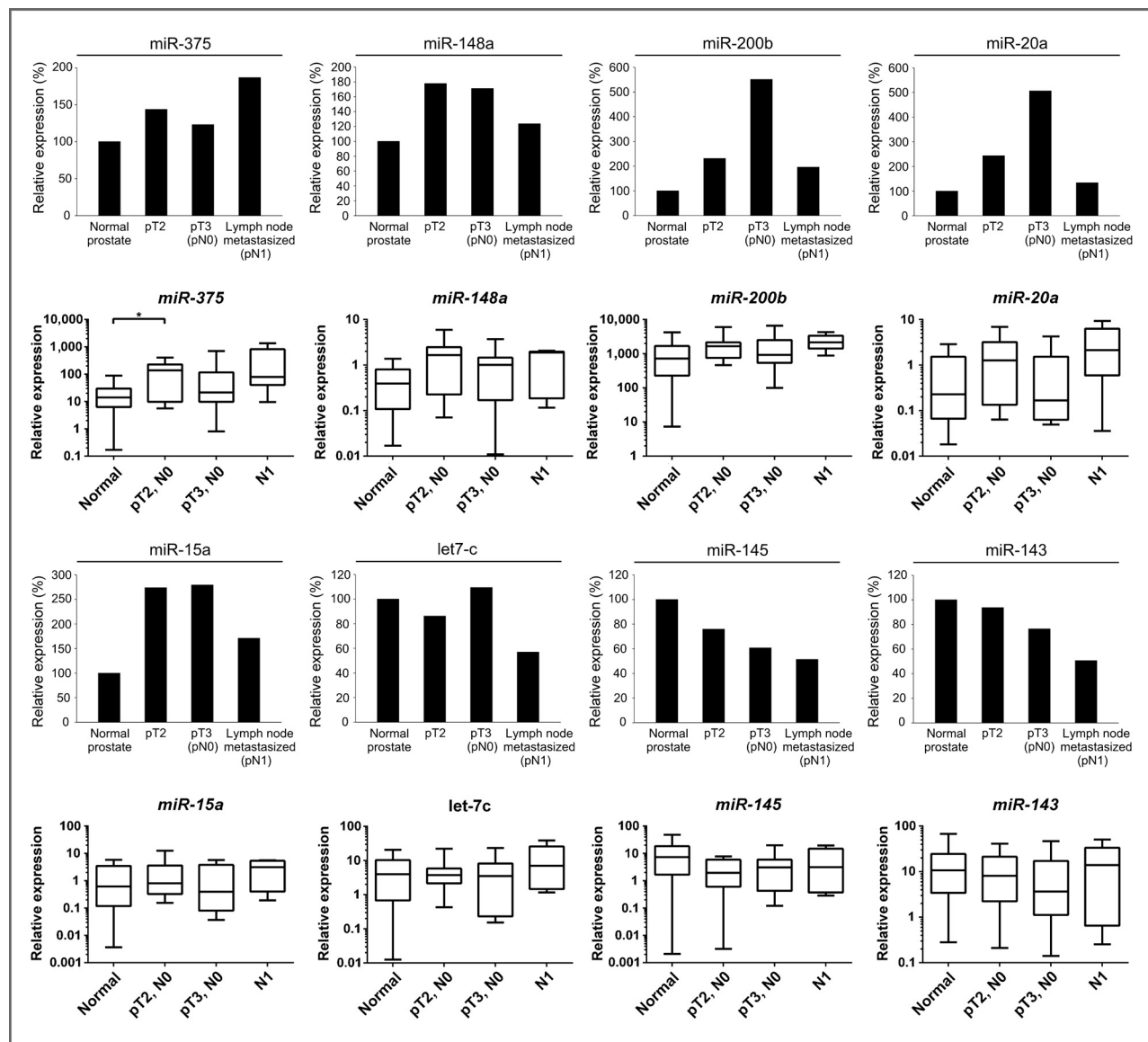


Figure 2. Validation of the miRNA expression profile by quantification of Northern blotting and qRT-PCR. The expression of eight miRNAs was assessed by Northern blotting in pooled RNA preparations (black bars) and by qRT-PCR in 40 pairs of tumor tissue and corresponding normal tissue (box and whisker plots).

metastasizing samples (pN1). We point out that *miR-375* is increased in all tumor samples by sequencing, Northern blotting, and qRT-PCR. The initial increase of *miR-200b* and *miR-20a* levels observed from normal to the pT2 (pN0) to pT3 (pN0) cases, followed by a decrease in the lymph node metastasizing cases, were confirmed by Northern blotting but not by qRT-PCR.

For *miR-15a*, we found by sequencing an increase in all tumor entities. In the Northern blots, the level dropped from pT3 (pN0) to pN1 but was still higher than in a normal tissue. This increase was not confirmed by qRT-PCR (Fig. 2).

For *miR-145*, by sequencing, we found a stepwise decrease in the expression from normal to pT2, pT3, and pN1 samples. The identical regulation pattern was observed in Northern blotting but could not be confirmed in qRT-PCR. For *miR-143*, we observed by sequencing an analogous reduction in expression from normal to pT2 to pT3 tumors but no further reduction in pN1 samples. The Northern blot analysis, however, displayed in addition a continuous reduction from pT3 to pN1 samples but this regulation could not be confirmed in qRT-PCR. For *let-7c*, we detected by sequencing and Northern blotting a decreased expression in pT2 tumors, an increase even above the expression levels in normal tissue for pT3 tumors with a subsequent and strong decrease in expression in pN1 tumors but this regulation could not be confirmed in qRT-PCR. For *miR-148a*, both by sequencing and Northern blotting, we detected an increase in the expression from normal to pT2 to pT3 tumors. The sequencing analysis indicated a further increase in pN1 tumors whereas the Northern blotting analysis suggested a reduction in pN1 tumors, but this regulation could not be confirmed in qRT-PCR.

SEC23A* is a target for *miR-200b

The *SEC23A* mRNA is a target for both *miR-200c* and *miR-375* (9, 21). The 3'UTR of the *SEC23A* mRNA has two predicted binding sites (Fig. 3A), which are identical for *miR-200b* and *miR-200c*. We could previously show that *miR-200c* functionally interacts with one of these binding sites (9). In the present analysis, we found an upregulation of *miR-200b*, which shares the seed sequence with *miR-200c*. The reporter gene experiments confirmed a negative regulatory effect of *miR-200b* on the *SEC23A* 3'UTR (Fig. 3A). The site-directed mutation of the two predicted miRNA binding sites revealed that only one of them, the binding site which we could confirm to be a target of *miR-200c*, is also the target site for *miR-200b* (nt 855, Fig. 3A). Ectopic expression of *miR-200b* in LNCaP or DU145 prostate carcinoma cells resulted in a 40% downregulation of the *SEC23A* protein (Fig. 4A). The expression of *miR-200b* was verified by Northern blotting (Supplementary Fig. S2A and S2B).

***PHLPP1* and *PHLPP2* are targets for *miR-15a* and *miR-375*, respectively**

In both our previous and the present analyses, *miR-375* exhibited the strongest upregulation of all miRNAs in the

prostate carcinoma samples. The TargetScan v4.1 prediction algorithm identified *PHLPP1* as a high-ranked target for *miR-375*. *PHLPP1* is recognized as a tumor suppressor with a prominent role in suppressing oncogenic signaling pathways, including the AKT pathway (for review, see refs. 22, 23). Interestingly, another member of this family of phosphatases, *PHLPP2*, is a potential target of *miR-15a*, which we found to be upregulated in deep sequencing and Northern blotting in all prostate carcinoma samples. Therefore, we performed reporter gene analyses to test whether both *PHLPP* genes are targets of miRNAs deregulated in prostate carcinoma. For both, the *PHLPP1* (Fig. 3B) and *PHLPP2* (Fig. 3C) 3'UTRs, we observed a significant reduction in reporter gene activity when coexpressed with the respective miRNAs. The expression construct for *miR-375* was previously described (Supplementary data in ref. 5); the ectopic expression of *miR-15a* from the corresponding pSG5 construct is shown by Northern blotting Supplementary Fig. S3A. The binding sites (seed sequences) for the two miRNAs were subsequently mutated, and we could show that the mutated reporter gene constructs were no more responsive to the corresponding miRNAs (Fig. 3B and C). The two miRNAs were then overexpressed in DU145 and LNCaP prostate carcinoma cells, and the protein expression of *PHLPP1* or *PHLPP2* was determined by Western blotting. As shown in Fig. 4B, *miR-375* reduced the levels of *PHLPP1* in DU145 and LNCaP cells to 60% as compared with the controls. Likewise, we observed a 40% reduction of *PHLPP2* by *miR-15a* (Fig. 4C).

To corroborate the above findings, we assessed the expression of the *SEC23A*, *PHLPP1*, and *PHLPP2* mRNAs in primary prostate carcinoma samples and the corresponding normal tissue. As shown in Supplementary Fig. S4, the *PHLPP2* mRNA was significantly reduced from normal to pT2 prostate carcinoma, whereas the *SEC23A* and the *PHLPP1* mRNAs were expressed at lower levels in the tumor samples. However, this reduction did not reach significance.

Coexpression of *miR-15a* and *miR-375* increases the growth of prostate carcinoma cell lines

As it is known that *PHLPP* protein phosphatases are potent inhibitors of proliferative signaling pathways, we tested the effects of *miR-15a* and *miR-375* overexpression on the proliferation of prostate carcinoma cell lines. Both miRNAs were overexpressed either alone or combined in the LNCaP and DU145 cell lines. For *miR-375*, we had previously shown that its expression is increased in DU145 and LNCaP prostate carcinoma cell lines as compared with prostate normal fibroblasts (PNFs; Fig. 3 in Szczyrba and colleagues; ref. 5). The endogenous level of *miR-15a* in PNFs versus the DU145 and LNCaP cell lines is shown in Supplementary Fig. S3B. As can be seen in Fig. 5A, the coexpression of *miR-15a* and *miR-375* significantly enhanced cell proliferation of both cell lines ($P < 0.001$; two-way ANOVA). We also inhibited the expression of *miR-15a* and *miR-375* using antisense

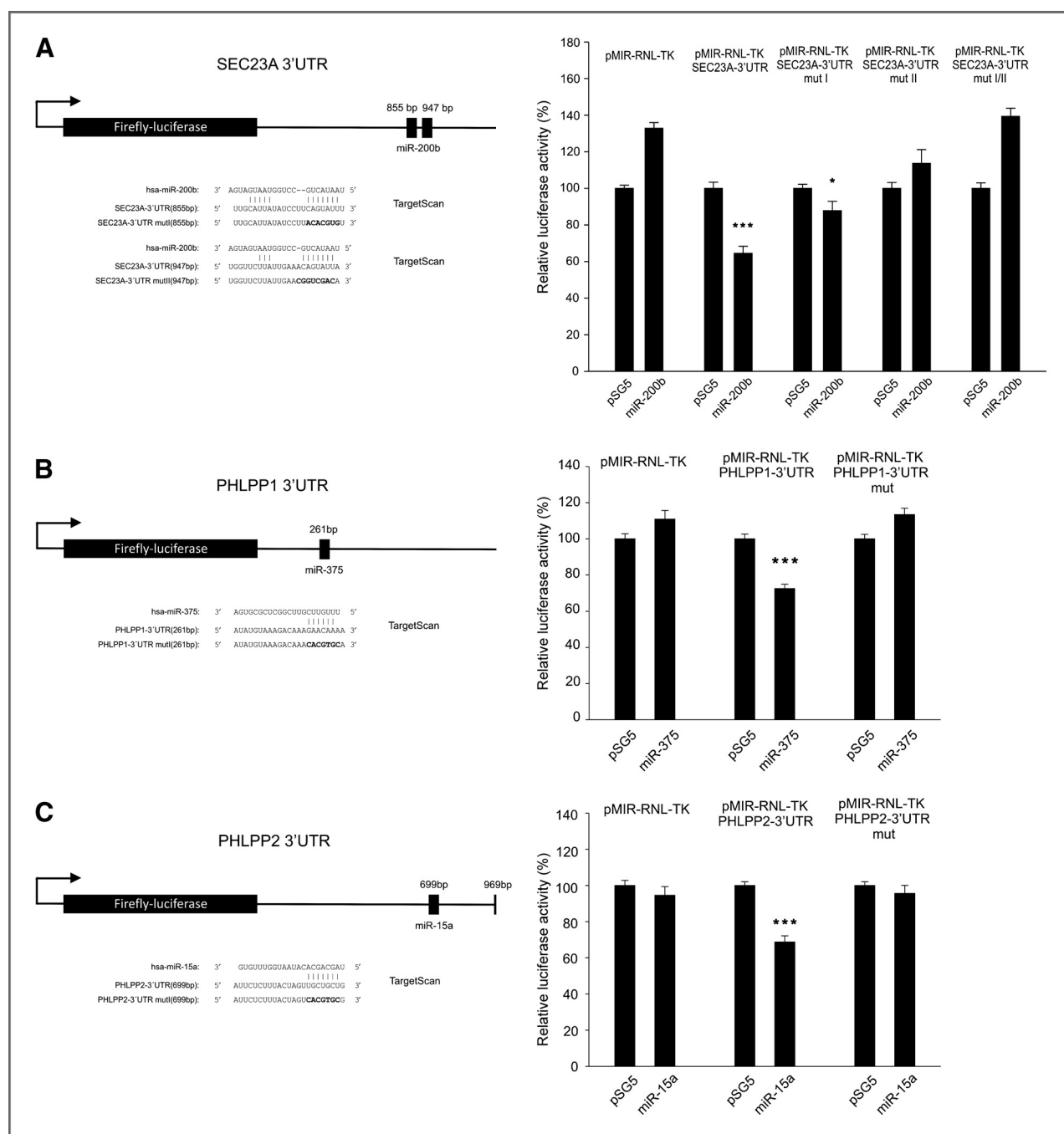
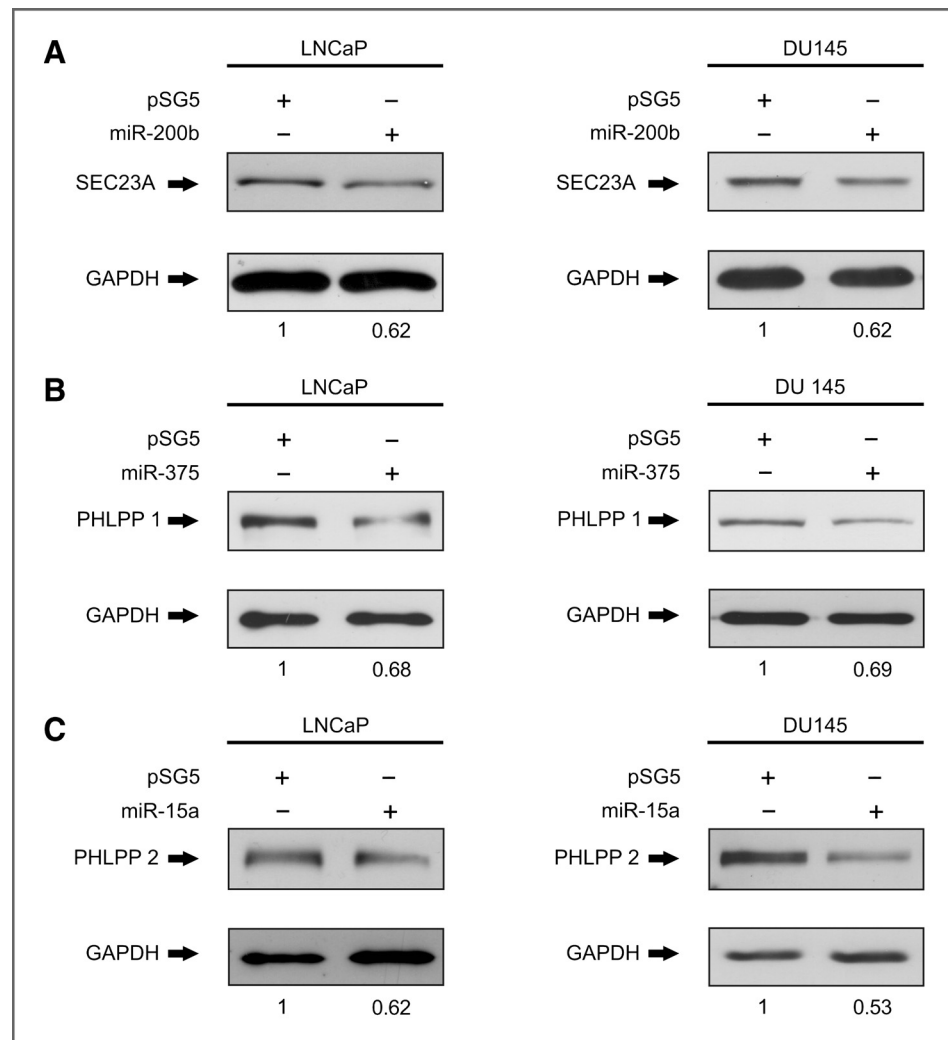


Figure 3. Luciferase reporter gene assays. For the 3'UTR regions of *SEC23A* (A), *PHLPP1* (B), and *PHLPP2* (C), a schematic representation of the reporter gene construct with the predicted miRNA interaction site, as well as the mutated interaction site, is shown. The reporter gene constructs were expressed with or without miRNA-expression constructs in the indicated combinations. Results represent the mean of four independent experiments performed in duplicates. ***, $P < 0.001$.

oligonucleotides. As shown in Fig. 5B, the joint knock-down of *miR-15a* and *miR-375* reduced cell proliferation after 72 hours ($P < 0.0001$; two-way ANOVA). As LNCaP cells do not express appreciable amounts of *miR-375* (5), we only carried out a knockdown experiment in DU145 cells. We noticed a reduction of cell growth at the 72-hour time point when the empty pSG5

vector was transfected into the DU145 cells (Fig. 5A). Additional experiments confirmed that this represents a specific effect of the pSG5 control vector in DU145 cells (Supplementary Fig. S5). However, the cotransfection of *miR-15* and *miR-375* in DU145 cells clearly leads to an induction of cell growth compared with the empty control vector and the single transfections.

Figure 4. Regulation of SEC23A, PHLPP1, and PHLPP2 protein expression by *miR-200b*, *miR-375*, and *miR-15a*. The prostate cancer cell lines LNCaP and DU145 were transfected either with control or the adequate miRNA expression vectors as mentioned in the figure. Forty-eight hours after transfection of the cell lines, the protein expression of SEC23A (A), PHLPP1 (B), and PHLPP2 (C) was analyzed by Western blotting. The quantification of the Western blots represent the relative downregulation that was determined in three independent experiments using GAPDH as loading control.



Discussion

The results presented in this manuscript confirm and extend our previous miRNA-expression profiling carried out by high-throughput sequencing (5). The comparison of the samples derived from the corresponding nonmalignant tissue adjacent to prostate carcinoma and healthy prostate tissue derived from cystectomy specimens yielded essentially the same expression profiles as previously described for corresponding normal prostate tissue (5). Likewise, the majority of all deregulated miRNAs were repeatedly found in this analysis, indicating that the methods yield reproducible results. The overall expression of *miR-375* increased in the tumor samples compared with normal tissue irrespective of the tumor stage. We found an initial increase from normal to pT2 (pN0), then a slight drop from pT2 (pN0) to pT3 (pN0), and then a strong increase in the pN1 samples. This increase in *miR-375* was initially reported in our earlier study (5), as well as by Schaefer and colleagues (24) and Martens-Uzunova and colleagues (25). Two recent studies reported increased serum levels of *miR-375* (and *miR-141*) in patients with metastatic prostate carcinoma

(26, 27). In contrast, a miRNA profiling approach based on high-throughput sequencing by Watahiki and colleagues did not find an increase of *miR-375* in metastatic prostate carcinoma (28). Other studies using microarray analysis also did not find an induction of *miR-375* in prostate carcinoma (reviewed in refs. 3 and 29). However, we were able to verify our deep sequencing analysis by Northern blotting analysis. By sequencing, the levels of *miR-200b* and *miR-200c* gradually increased with the malignancy of the samples but then dropped to lower levels in the metastasizing samples. This observation was confirmed for *miR-200b* by Northern blotting analysis of the samples used for the generation of the cDNA libraries. Using a set of 40 corresponding pairs of primary tumor samples and the nonmalignant tissues, we observed an increase in all tumor samples for *miR-200b*. Future experiments employing larger numbers of cases will have to be carried out to address this issue. The significance of *miR-200b/c* overexpression as found here is highlighted by the fact that the overexpression of *miR-200* induced migration in PC3 cells (30) and that downregulation of SEC23A by *miR-200c* has been described as

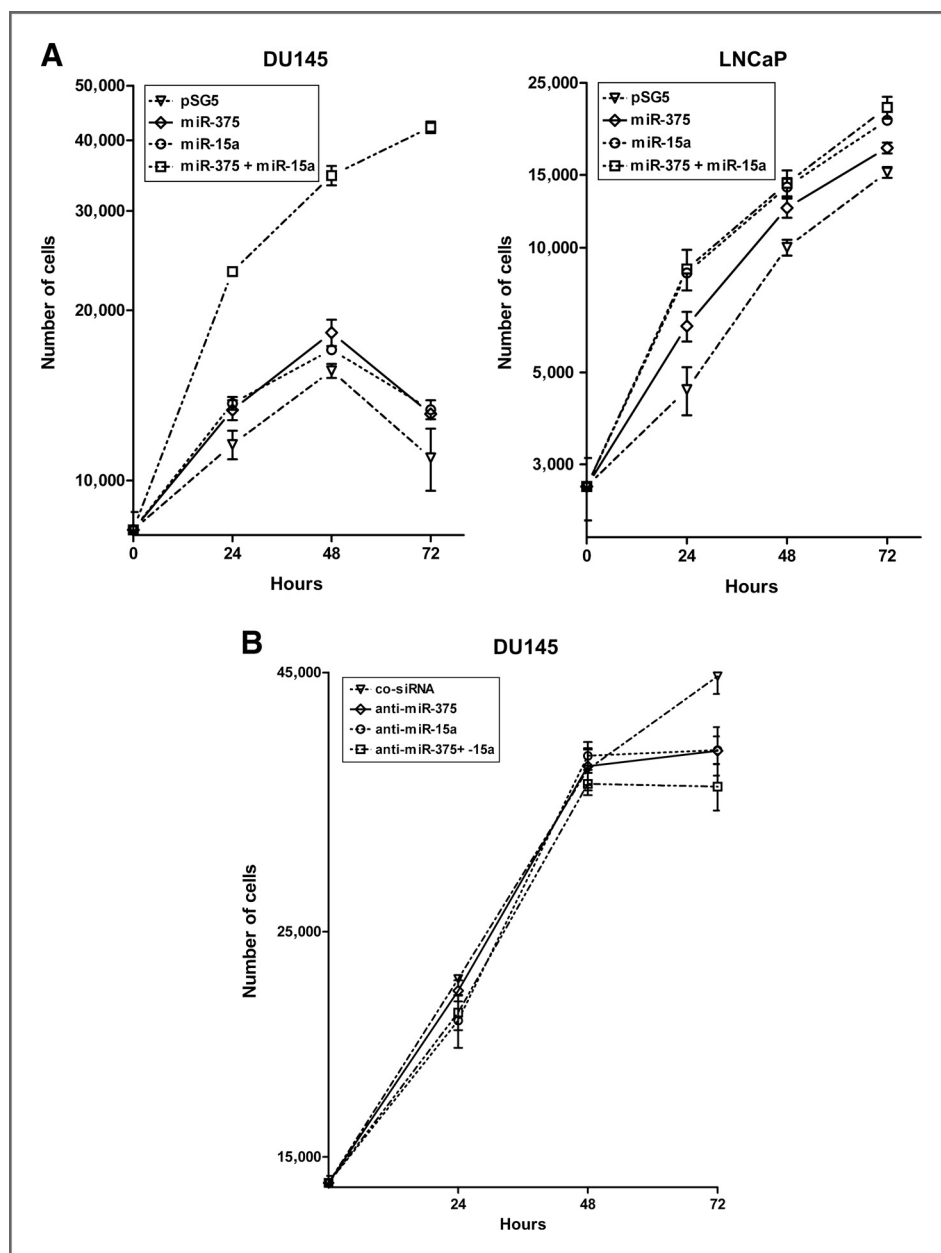


Figure 5. Coexpression of *miR-375* and *miR-15a* promotes growth of prostate carcinoma cell lines. A, DU145 or LNCaP cells were transfected either with control vector or miRNA expression vectors. The cells were harvested and counted by fluorescence-activated cell sorting (FACS) analysis at the indicated time points. B, DU145 cells were transfected either with control siRNA or miRNA inhibitors and counted by FACS analysis at the indicated time points. The proliferation assays were carried out in triplicate. Bars represent the standard error of the mean.

a metastasis-promoting event (31), corroborated by our finding that *SEC23A* is also a target for *miR-375* (9). Our observation that *miR-200b* and *miR-200c* first increase in their expression with the stage of malignancy but then decrease with progression to a metastasizing tumor would be in line with their proposition that there is a shift in *SEC23A* levels from nonmetastatic to metastatic tumors (21). In addition, Kong and colleagues showed that the *miR-200* family regulates epithelial–mesenchymal transition, adhesion, and invasion of prostate cancer cells which are characteristic features of metastatic cells (32).

Recent data also describe elevated serum levels of *miR-375* and *miR-141* as predictors for poor prognosis (27) or metastasis (26) reviewed in reference 6. *MiR-141* is found

upregulated in primary tissues in a variety of studies including ours (2, 25), and inclusion of miRNA expression data significantly improves the accuracy of markers like prostate-specific antigen in the diagnosis or prediction of tumor outcome (33). The induction of the *miR-106b-93-25* cluster is in line with the poor prognosis described by others (34). Previously, *miR-190* was shown to downregulate *PHLPP1* (35). In our analysis, *miR-190* was not deregulated in the different stages of prostate carcinoma that were analyzed. Instead, we found that *miR-375* and *miR-15a* coordinately downregulate *PHLPP1* and *PHLPP2*, respectively. Genomic deletion of the *PHLPP1* and *PHLPP2* genes was described as being correlated with the induction of prostate carcinoma (11–13) and a *PTEN/PHLPP1* knockout mouse

develops prostate carcinoma with a high penetrance (12). A downregulation of PHLPP1 or PHLPP2 could be detected in 11% of primary prostate carcinoma and in 37% of metastases (23, 36). Recently, it has been reported that both *PHLPP1* and *PHLPP2* are deleted or downregulated in combination with highly metastatic prostate carcinoma (22) or glioblastoma (37). PHLPPs belong to a family of phosphatases that regulate protein kinases A, B (known as Akt), and C and ribosomal protein S6 kinase (RPS6K) negatively (23, 38). PHLPP1 and PHLPP2 are considered to be tumor suppressors because they suppress cell survival, both by inhibiting proliferative pathways and by promoting apoptotic pathways (23). PHLPP in membrane rafts of rat brains can negatively regulate the proliferative RAS–mitogen-activated protein kinase (MAPK) pathway (39). Furthermore, human PHLPP1 and PHLPP2 can differentially regulate proliferative AKT signaling by selectively dephosphorylating the hydrophobic motifs of AKT2 or AKT3. Knockdown of PHLPP1 specifically modulated phosphorylation of human double minute 2 (HDM2) and glycogen synthetase kinase 3 alpha (GSK3A) through AKT2, and PHLPP2 specifically modulated phosphorylation of p27 (CDKN1B) through AKT3 (40). On the other hand, PHLPP can act proapoptotic; when inactivating AKT, it catalyzes an activating dephosphorylation of the proapoptotic kinase MST1 (the human homologue of Hippo; 41, 42). Altogether, PHLPPs affect major cancer pathways as RAS–MAPK, ABC protein kinases, and p53 (via HDM2 and p27) signaling, which have been described as also being significant in prostate cancer (23, 43).

The induction of *miR-375* and *miR-15a* can contribute to the downregulation of PHLPPs activity in prostate carcinoma. Although several studies did not notice an upregulation of *miR-375* in prostate carcinoma samples, various studies observed increased levels of this miRNA in prostate cancer serum samples (44, 45). Publications confirm that *miR-375* is downregulated in other cancer types such as cervical, lung, or head and neck carcinoma, as well as glioma (46–50) but upregulated in breast carcinoma (51). Likewise, *miR-15a* was previously shown to be downregulated in metastasizing prostate carcinoma (18). We observed an initial upregulation and a subsequent downregulation of *miR-15a* in the metastatic samples, albeit at levels above those detected in normal tissue. In two studies, an increase of *miR-15a* was found to be of negative predictive value in renal cell carcinoma (52) or diffuse large B-cell lymphoma (53). There are now large numbers of studies that established miRNA profiles of prostate carcinoma, which, to some extent, report conflicting results (reviewed in ref. 3). Our observation that *miR-15a* is increased in the different tumor stages examined is in contradiction with data presented by Bonci and colleagues, which described a downregulation of *miR-15a* in prostate carcinoma (18) in line with the notion that *miR-15a* (and *miR-16*) are tumor-suppressor miRNAs. Our previous study on intermediately aggressive prostate carcinoma (5) with Gleason scores of 6 or 7 yielded an upregulation in one and a downregulation in the parallel patient cohort (5). Our qRT-PCR analysis, however, showed a slight increase in

miR-15a expression, which was not statistically significant though various other studies did not find a significant deregulation of *miR-15a* (34, 54, 55). The study by Ambs found an upregulation of miR-16, also at odds with the report by Bonci and colleagues (18). However, *miR-15a* is considered as tumor suppressor at inducing cell cycle arrest and apoptosis in prostate carcinoma (reviewed in ref. 6). A recent review on miRNAs and their influence on functional protein networks also predicted that *miR-15a* plays an inhibitory role for prostate cancer cell growth (56). We find that 10/21 miRNAs predicted in that publication (see, i.e., Fig. 3 in ref. 56) to play a role in tumorigenesis were also found in our analysis. This implies that a large number of bioinformatical predictions may be experimentally validated. There are different explanations for the often inconsistent results about *miR-15a*, in that they could be due to different methods employed, such as qRT-PCR, microarray, or cDNA sequencing.

Altogether, miRNA profiling of pT2 (pN0), pT3 (pN0), and lymph node metastasizing prostate carcinoma (pN1) by deep sequencing revealed clearly changed miRNA levels. Two miRNAs, *miR-375* and *miR-15a* with high levels at all tumor stages detected by deep sequencing and Northern blotting, target the phosphatases *PHLPP1* and *PHLPP2*, respectively. Both phosphatases PHLPP1 and PHLPP2 normally suppress survival pathways as AKT- and RAS–MAPK, which are abrogated in prostate carcinoma. Overexpression of *miR-15a* and *miR-375* results in a downregulation of PHLPP1/2 and an increase in prostate carcinoma cell growth. Our results disclose an association between miRNA regulation and major phosphatase pathways in prostate carcinoma development.

Disclosure of Potential Conflicts of Interest

No potential conflicts of interest were disclosed.

Authors' Contributions

Conception and design: M. Hart, S. Wach, F.A. Grässer, B. Wullich

Development of methodology: T.T. Rau

Acquisition of data (provided animals, acquired and managed patients, provided facilities, etc.): S. Wach, T.T. Rau, A. Hartmann, B. Wullich

Analysis and interpretation of data (e.g., statistical analysis, biostatistics, computational analysis): M. Hart, E. Nolte, S. Wach, J. Szczyrba, H. Taubert, T.T. Rau, F.A. Grässer, B. Wullich

Writing, review, and/or revision of the manuscript: M. Hart, E. Nolte, S. Wach, H. Taubert, A. Hartmann, F.A. Grässer, B. Wullich

Administrative, technical, or material support (i.e., reporting or organizing data, constructing databases): T.T. Rau, A. Hartmann

Study supervision: S. Wach, J. Szczyrba, F.A. Grässer, B. Wullich

Acknowledgments

The authors thank Ruth Nord for expert technical assistance and Gabrielle P. Cooper (MA) for language-editing service.

Grant Support

This work was supported by the Wilhelm-Sander-Stiftung by a grant 2007.025.01 (to B. Wullich and F.A. Grässer).

The costs of publication of this article were defrayed in part by the payment of page charges. This article must therefore be hereby marked *advertisement* in accordance with 18 U.S.C. Section 1734 solely to indicate this fact.

Received May 8, 2013; revised October 21, 2013; accepted November 6, 2013; published OnlineFirst December 13, 2013.

References

1. Ferlay J, Shin HR, Bray F, Forman D, Mathers C, Parkin DM. Estimates of worldwide burden of cancer in 2008: GLOBOCAN 2008. *Int J Cancer* 2010;127:2893–917.
2. Coppola V, De Maria R, Bonci D. MicroRNAs and prostate cancer. *Endocr Relat Cancer* 2010;17:F1–17.
3. Maugeri-Sacca M, Coppola V, Bonci D, De Maria R. MicroRNAs and prostate cancer: from preclinical research to translational oncology. *Cancer J (Sudbury, Mass)* 2012;18:253–61.
4. Meister G. miRNAs get an early start on translational silencing. *Cell* 2007;131:25–8.
5. Szczyrba J, Loprich E, Wach S, Jung V, Unteregger G, Barth S, et al. The MicroRNA profile of prostate carcinoma obtained by deep sequencing. *Mol Cancer Res* 2010;8:529–38.
6. Fang YX, Gao WQ. Roles of microRNAs during prostatic tumorigenesis and tumor progression. *Oncogene* 2013 Mar 4. doi:10.1038/onc.2013.54
7. O'Kelly F, Marignol L, Meunier A, Lynch TH, Perry AS, Hollywood D. MicroRNAs as putative mediators of treatment response in prostate cancer. *Nat Rev Urol* 2012;9:397–407.
8. Wach S, Nolte E, Szczyrba J, Stöhr R, Hartmann A, Ørntoft T, et al. MiRNA profiles of prostate carcinoma detected by multi-platform miRNA screening. *Int J Cancer* 2011;130:611–21.
9. Szczyrba J, Nolte E, Wach S, Kremmer E, Stöhr R, Hartmann A, et al. Downregulation of Sec23A protein by miRNA-375 in prostate carcinoma. *Mol Cancer Res* 2011;9:791–800.
10. Szczyrba J, Nolte E, Hart M, Döll C, Wach S, Taubert H, et al. Identification of ZNF217, hnRNP-K, VEGF-A and IPO7 as targets for microRNAs that are downregulated in prostate carcinoma. *Int J Cancer* 2013;132:775–84.
11. Mulholland DJ, Tran LM, Li Y, Cai H, Morim A, Wang S, et al. Cell autonomous role of PTEN in regulating castration-resistant prostate cancer growth. *Cancer Cell* 2011;19:792–804.
12. Chen M, Pratt CP, Zeeman ME, Schultz N, Taylor BS, O'Neill A, et al. Identification of PHLPP1 as a tumor suppressor reveals the role of feedback activation in PTEN-mutant prostate cancer progression. *Cancer Cell* 2011;20:173–86.
13. Carver BS, Chapinski C, Wongvipat J, Hieronymus H, Chen Y, Chandralapathy S, et al. Reciprocal feedback regulation of PI3K and androgen receptor signaling in PTEN-deficient prostate cancer. *Cancer Cell* 2011;19:575–86.
14. Wittekind C, Compton CC, Greene FL, Sobin LH. TNM residual tumor classification revisited. *Cancer* 2002;94:2511–6.
15. Ozen M, Creighton CJ, Ozdemir M, Ittmann M. Widespread deregulation of microRNA expression in human prostate cancer. *Oncogene* 2008;27:1788–93.
16. Porkka KP, Pfeiffer MJ, Waltering KK, Vessella RL, Tammela TL, Visakorpi T. MicroRNA expression profiling in prostate cancer. *Cancer Res* 2007;67:6130–5.
17. Boll K, Reiche K, Kasack K, Mörbt N, Kretzschmar AK, Tomm JM, et al. MiR-130a, miR-203 and miR-205 jointly repress key oncogenic pathways and are downregulated in prostate carcinoma. *Oncogene* 2013;32:277–85.
18. Bonci D, Coppola V, Musumeci M, Addario A, Giuffrida R, Memeo L, et al. The *miR-15a*-miR-16-1 cluster controls prostate cancer by targeting multiple oncogenic activities. *Nat Med* 2008;14:1271–7.
19. Fujita Y, Kojima K, Ohhashi R, Hamada N, Nozawa Y, Kitamoto A, et al. MiR-148a attenuates paclitaxel resistance of hormone-refractory, drug-resistant prostate cancer PC3 cells by regulating MSK1 expression. *J Biol Chem* 2010;285:19076–84.
20. Murata T, Takayama K, Katayama S, Urano T, Horie-Inoue K, Ikeda K, et al. *miR-148a* is an androgen-responsive microRNA that promotes LNCaP prostate cell growth by repressing its target CAND1 expression. *Prostate Cancer Prostatic Dis* 2010;13:356–61.
21. Korpala M, Eil BJ, Buffa FM, Ibrahim T, Blanco MA, Celià-Terrassa T, et al. Direct targeting of Sec23a by miR-200s influences cancer cell secretome and promotes metastatic colonization. *Nat Med* 2011;17:1101–8.
22. Warfel NA, Newton AC. Pleckstrin homology domain leucine-rich repeat protein phosphatase (PHLPP): a new player in cell signaling. *J Biol Chem* 2012;287:3610–6.
23. O'Neill AK, Niederst MJ, Newton AC. Suppression of survival signalling pathways by the phosphatase PHLPP. *FEBS J* 2013;280:572–83.
24. Schaefer A, Jung M, Mollenkopf HJ, Wagner I, Stephan C, Jentzmik F, et al. Diagnostic and prognostic implications of microRNA profiling in prostate carcinoma. *Int J Cancer* 2010;126:1166–76.
25. Martens-Uzunova ES, Jalava SE, Dits NF, van Leenders GJ, Møller S, Trapman J, et al. Diagnostic and prognostic signatures from the small non-coding RNA transcriptome in prostate cancer. *Oncogene* 2012;31:978–91.
26. Bryant RJ, Pawlowski T, Catto JW, Marsden G, Vessella RL, Rhee S, et al. Changes in circulating microRNA levels associated with prostate cancer. *Br J Cancer* 2012;106:768–74.
27. Nguyen HC, Xie W, Yang M, Hsieh CL, Drouin S, Lee GS, et al. Expression differences of circulating microRNAs in metastatic castration resistant prostate cancer and low-risk, localized prostate cancer. *Prostate* 2013;73:346–54.
28. Watahiki A, Wang Y, Morris J, Dennis K, O'Dwyer HM, Gleave M, et al. MicroRNAs associated with metastatic prostate cancer. *PLoS ONE* 2011;6:e24950.
29. Sorensen KD, Ørntoft TF. Discovery of prostate cancer biomarkers by microarray gene expression profiling. *Expert Rev Mol Diagn* 2010;10:49–64.
30. Virtakoivu R, Pellinen T, Rantala JK, Perala M, Ivaska J. Distinct roles of AKT isoforms in regulating beta1-integrin activity, migration, and invasion in prostate cancer. *Mol Biol Cell* 2012;23:3357–69.
31. Korpala M, Lee ES, Hu G, Kang Y. The miR-200 family inhibits epithelial-mesenchymal transition and cancer cell migration by direct targeting of E-cadherin transcriptional repressors ZEB1 and ZEB2. *J Biol Chem* 2008;283:14910–4.
32. Kong D, Li Y, Wang Z, Banerjee S, Ahmad A, Kim HR, et al. miR-200 regulates PDGF-D-mediated epithelial-mesenchymal transition, adhesion, and invasion of prostate cancer cells. *Stem Cells (Dayton, Ohio)* 2009;27:1712–21.
33. Gonzales JC, Fink LM, Goodman OB Jr., Symanowski JT, Vogelzang NJ, Ward DC. Comparison of circulating MicroRNA 141 to circulating tumor cells, lactate dehydrogenase, and prostate-specific antigen for determining treatment response in patients with metastatic prostate cancer. *Clin Genitourin Cancer* 2011;9:39–45.
34. Ambs S, Prueitt RL, Yi M, Hudson RS, Howe TM, Petrocca F, et al. Genomic profiling of microRNA and messenger RNA reveals deregulated microRNA expression in prostate cancer. *Cancer Res* 2008;68:6162–70.
35. Beezhold K, Liu J, Kan H, Meighan T, Castranova V, Shi X, et al. miR-190-mediated downregulation of PHLPP contributes to arsenic-induced Akt activation and carcinogenesis. *Toxicol Sci* 2011;123:411–20.
36. Taylor BS, Schultz N, Hieronymus H, Gopalan A, Xiao Y, Carver BS, et al. Integrative genomic profiling of human prostate cancer. *Cancer Cell* 2010;18:11–22.
37. Molina JR, Agarwal NK, Morales FC, Hayashi Y, Aldape KD, Cote G, et al. PTEN, NHERF1 and PHLPP form a tumor suppressor network that is disabled in glioblastoma. *Oncogene* 2011;31:1264–74.
38. Newton AC. Regulation of the ABC kinases by phosphorylation: protein kinase C as a paradigm. *Biochem J* 2003;370 (Pt 2):361–71.
39. Shimizu K, Okada M, Nagai K, Fukada Y. Suprachiasmatic nucleus circadian oscillatory protein, a novel binding partner of K-Ras in the membrane rafts, negatively regulates MAPK pathway. *J Biol Chem* 2003;278:14920–5.
40. Brognard J, Sierrecki E, Gao T, Newton AC. PHLPP and a second isoform, PHLPP2, differentially attenuate the amplitude of Akt signaling by regulating distinct Akt isoforms. *Mol Cell* 2007;25:917–31.
41. Jang SW, Yang SJ, Srinivasan S, Ye K. Akt phosphorylates Mst1 and prevents its proteolytic activation, blocking FOXO3

- phosphorylation and nuclear translocation. *J Biol Chem* 2007; 282:30836–44.
42. Qiao M, Wang Y, Xu X, Lu J, Dong Y, Tao W, et al. Mst1 is an interacting protein that mediates PHLPPs' induced apoptosis. *Mol Cell* 2010; 38:512–23.
 43. Mimeault M, Batra SK. Frequent gene products and molecular pathways altered in prostate cancer- and metastasis-initiating cells and their progenies and novel promising multi-targeted therapies. *Mol Med (Cambridge, Mass)* 2011;17: 949–64.
 44. Fendler A, Stephan C, Yousef GM, Jung K. MicroRNAs as regulators of signal transduction in urological tumors. *Clin Chem* 2011; 57:954–68.
 45. Zhang X, Yan Z, Zhang J, Gong L, Li W, Cui J, et al. Combination of hsa-miR-375 and hsa-miR-142-5p as a predictor for recurrence risk in gastric cancer patients following surgical resection. *Ann Oncol* 2011; 22:2257–66.
 46. Ding L, Xu Y, Zhang W, Deng Y, Si M, Du Y, et al. MiR-375 frequently downregulated in gastric cancer inhibits cell proliferation by targeting JAK2. *Cell Res* 2010;20:784–93.
 47. Tsukamoto Y, Nakada C, Noguchi T, Tanigawa M, Nguyen LT, Uchida T, et al. MicroRNA-375 is downregulated in gastric carcinomas and regulates cell survival by targeting PDK1 and 14-3-3zeta. *Cancer Res* 2010;70:2339–49.
 48. Ladeiro Y, Couchy G, Balabaud C, Bioulac-Sage P, Pelletier L, Rebouissou S, et al. MicroRNA profiling in hepatocellular tumors is associated with clinical features and oncogene/tumor suppressor gene mutations. *Hepatology* 2008;47:1955–63.
 49. Avissar M, Christensen BC, Kelsey KT, Marsit CJ. MicroRNA expression ratio is predictive of head and neck squamous cell carcinoma. *Clin Cancer Res* 2009;15:2850–5.
 50. Mathe EA, Nguyen GH, Bowman ED, Zhao Y, Budhu A, Schetter AJ, et al. MicroRNA expression in squamous cell carcinoma and adenocarcinoma of the esophagus: associations with survival. *Clin Cancer Res* 2009;15:6192–200.
 51. de Souza Rocha Simonini P, Breiling A, Gupta N, Malekpour M, Youns M, Omranipour R, et al. Epigenetically deregulated microRNA-375 is involved in a positive feedback loop with estrogen receptor alpha in breast cancer cells. *Cancer Res* 2010;70:9175–84.
 52. von Brandenstein M, Pandarakalam JJ, Kroon L, Loeser H, Herden J, Braun G, et al. MicroRNA 15a, inversely correlated to PKCalpha, is a potential marker to differentiate between benign and malignant renal tumors in biopsy and urine samples. *Am J Pathol* 2012;180: 1787–97.
 53. Fang C, Zhu DX, Dong HJ, Zhou ZJ, Wang YH, Liu L, et al. Serum microRNAs are promising novel biomarkers for diffuse large B cell lymphoma. *Ann Hematol* 2011;91:553–9.
 54. Volinia S, Calin GA, Liu CG, Ambs S, Cimmino A, Petrocca F, et al. A microRNA expression signature of human solid tumors defines cancer gene targets. *Proc Natl Acad Sci U S A* 2006;103:2257–61.
 55. Tong AW, Fulgham P, Jay C, Chen P, Khalil I, Liu S, et al. MicroRNA profile analysis of human prostate cancers. *Cancer Gene Ther* 2009;16:206–16.
 56. Alshalalfa M, Bader GD, Goldenberg A, Morris Q, Alhaji R. Detecting microRNAs of high influence on protein functional interaction networks: a prostate cancer case study. *BMC Syst Biol* 2012;6:112.